

LETTERS

Rotational breakup as the origin of small binary asteroids

Kevin J. Walsh^{1,2}, Derek C. Richardson² & Patrick Michel¹

Asteroids with satellites are observed throughout the Solar System, from subkilometre near-Earth asteroid pairs to systems of large and distant bodies in the Kuiper belt. The smallest and closest systems are found among the near-Earth and small inner main-belt asteroids, which typically have rapidly rotating primaries and close secondaries on circular orbits. About 15 per cent of near-Earth and main-belt asteroids with diameters under 10 km have satellites^{1,2}. The mechanism that forms such similar binaries in these two dynamically different populations was hitherto unclear. Here we show that these binaries are created by the slow spinup of a 'rubble pile' asteroid by means of the thermal YORP (Yarkovsky–O'Keefe–Radzievskii–Paddack) effect. We find that mass shed from the equator of a critically spinning body accretes into a satellite if the material is collisionally dissipative and the primary maintains a low equatorial elongation. The satellite forms mostly from material originating near the primary's surface and enters into a close, low-eccentricity orbit. The properties of binaries produced by our model match those currently observed in the small near-Earth and main-belt asteroid populations, including 1999 KW₄ (refs 3, 4).

The angular momentum content from the primary's rotation and the secondary's orbit among small binaries suggests that the satellites were formed by rotational disruption after the body was pushed beyond its critical spin limit^{2,5}. Tidal encounters can account for near-critical spin rates and are efficient at forming binaries from rubble piles; however, they are even more efficient at subsequently dissociating those binaries as a result of repeated planetary encounters^{6,7}. In the main belt, the catastrophic disruption of an asteroid can produce binary systems, but they do not match the observed properties of small binaries^{8,9}. Radar observations of binary near-Earth asteroid (NEA) 1999 KW₄ show that the primary is oblate with a pronounced equatorial belt, the effective gravity at the equator is directed inward but is nearly zero, and its equatorial elongation is nearly unity^{3,4}. Owing to the quality of the observations, and the diagnostic 'top-like' shape of the primary, this system is a key constraint for binary formation models. The small main-belt asteroid (SMBA) binaries have properties nearly identical to those of the NEA binaries, and both have an estimated frequency of ~15% (ref. 2). This suggests a common formation mechanism, which has not been identified so far.

One mechanism that operates on both NEAs and MBAs that may lead to the observed binaries is YORP-induced spinup, which arises from reflection and/or absorption and re-radiation of sunlight by the surface of an irregularly shaped asteroid^{10,11}. This effect accounts for the increase in the rotation rate of NEAs 2000 PH₅ and 1862 Apollo^{12–14}. The timescale for YORP spin alteration depends on the size R of the body (increasing with R^2), the distance a from the Sun (increasing with a^2), the body's thermal properties, and the

body's shape and obliquity. The YORP spinup/spindown timescale for kilometre-sized NEAs and MBAs is estimated to be between a few tens of thousands and a few million years, depending on the shape and makeup of the asteroid^{10,15}. Because of a notable abundance of both fast and slow rotators among NEAs and SMBAs, this effect seems to act widely¹⁶. However, it has never been shown whether gradual spinup leads to mass loss that can form binaries, and whether, if so, those binaries are a close match to observations.

We performed numerical simulations of YORP spinup of a cohesionless body consisting of ~1,000 self-gravitating rigid spheres. Several lines of evidence suggest that most kilometre-sized objects are rubble piles or gravitational aggregates, which means they lack cohesion but are non-fluid¹⁷. One indicator of the response of such bodies to stress is the angle of friction (ϕ) of the material. We modelled different kinds of rubble pile, ranging from a fluid-like body ($\phi \approx 0^\circ$), to a more typical terrestrial material ($\phi \approx 40^\circ$, here referred to as the nominal case)¹⁸. The model rubble piles consisted of either monodisperse spheres, or a simple bimodal distribution (meaning two different sizes of particles). Numerical experiments show that monodisperse rubble piles behave similarly to a body with $\phi \approx 40^\circ$, whereas ϕ for bimodal rubble piles depends on the relative particle sizes and their relative abundances within the body¹⁸. For our bimodal models, ϕ ranged from near 0° to $\sim 20^\circ$. We also tested another possible asteroid internal structure consisting of a rigid core of large particles surrounded by loose smaller particles. The representation of such a case by an angle of friction is not straightforward.

For the nominal case of $\phi \approx 40^\circ$, experiments were run with two different initial asteroid shapes: spherical and prolate. The prolate body had axis ratios of 2:1:1, and both shapes had initial spin periods of 4.4 h, longer than their stability limits for the body bulk density of 2.2 g cm^{-3} (where each particle had a density of 3.4 g cm^{-3}), so there was no immediate reshaping or collapsing. As the spin rate was increased (see below) and approached the critical spin limit, the spherical bodies became oblate, with mass moving from the poles to the equator. After this initial global reshaping of the spherical body, an equatorial belt of material remained, and subsequent mass loss originated from this region (Figs 1 and 2).

The fate of the ejected mass depends on the primary shape and the coefficient of restitution (the ratio of rebound to impact speed owing to energy dissipation when particles collide). In simulations with initially prolate bodies, the ejected mass does not readily accumulate into a satellite, because the mass that is ejected is lifted into a very shallow orbit barely above the surface of the primary and is easily disturbed by equatorial asymmetries in the prolate primary. In contrast, particles dislodged from spherical or oblate primaries quickly and efficiently accumulate into a satellite. For the most ideal parameters, namely $\phi \approx 40^\circ$ and a very low coefficient of restitution, the satellites accrete more than 90% of all ejected particles. In cases in which the primary

¹UMR 6202 Cassiopée, University of Nice-Sophia Antipolis, CNRS, Observatoire de la Côte d'Azur, BP 4229, 06304 Nice Cedex 4, France. ²Department of Astronomy, University of Maryland, College Park, Maryland 20742-2421, USA.

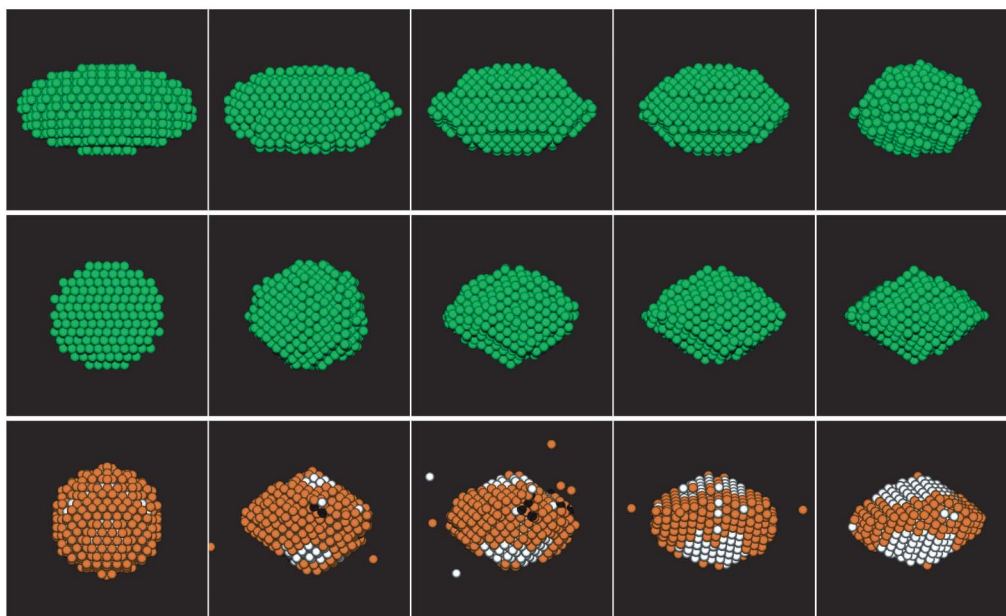


Figure 1 | Asteroid shape change during mass loss. The snapshots show the gradual change in shape that an initially prolate (top) and spherical (middle) body undergoes, as seen looking in the plane of the asteroid's equator. Also shown (bottom) is the movement and loss of a body's original surface particles (orange) and the exposure of the interior particles (white) during the binary formation. The top two rows show only the largest body in the simulation; ejected mass is not shown. Material that accumulates into a satellite does so slowly and from material lost from the equator of the

primary; there is no large-scale 'fission' event. The time between images is roughly 1,000 asteroid rotations for the top two rows, although for computational efficiency the simulations are sped up in comparison with the actual YORP effect. Prolate bodies become less elongated as particles are ejected from the ends of the long axis, reducing the critical rate for mass loss. Eventually prolate bodies become oblate, ending up with similar axis ratios to those of an initially spherical body.

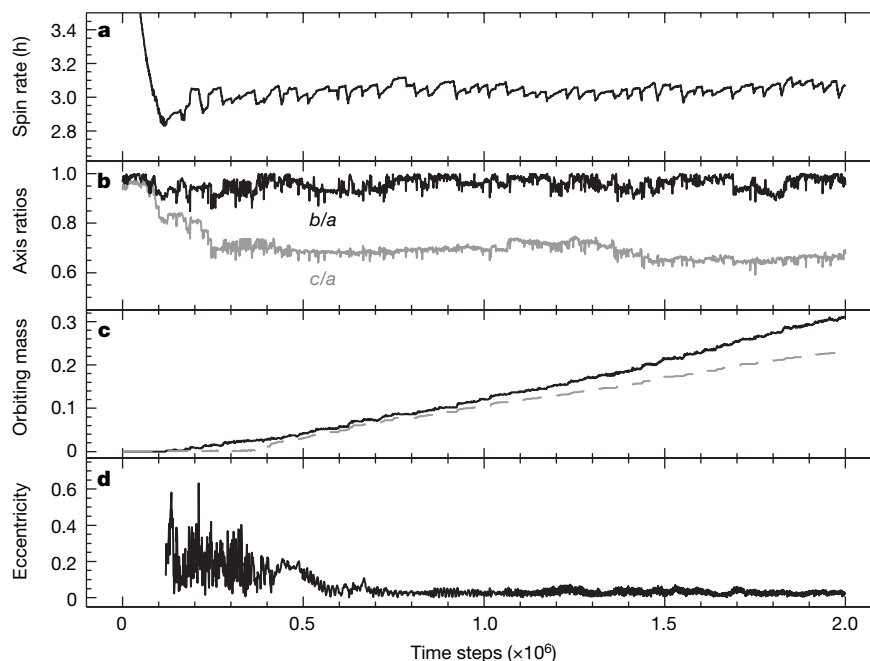


Figure 2 | Primary and secondary properties during satellite formation. **a**, Evolution of primary spin rate. **b**, Primary axis ratios (black, intermediate to long axis; grey, short to long axis). **c**, Mass loss (solid line) and satellite size (grey dashed line) as a fraction of progenitor mass. **d**, Satellite eccentricity. Plots are shown as a function of time steps of ~ 50 s. The originally spherical body becomes oblate after the increasing spin rate causes some mass loss. The newly oblate primary begins to accumulate mass in one satellite (dashed line in **c**), and the eccentricity quickly decreases to very low values. Initially prolate bodies show similar mass loss but do not accrete a satellite until

becoming oblate. The slow YORP spinup is modelled by applying small, discrete increases to the angular momentum of each particle making up the body, relative to the body's centre of mass. If any mass has been ejected or is in orbit, it is exempt from the angular momentum addition. The spin boosts are applied approximately every five rotation periods (for periods of ~ 3 h), allowing time for the body to equilibrate before more angular momentum is added to the system. If mass is lost between spin boosts, the next spin boost is delayed for at least about ten rotations, although these results were unchanged over a wide range of delay times between spin boosts.

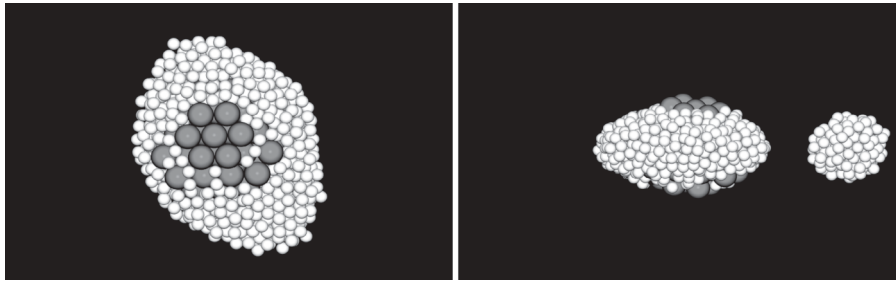


Figure 3 | Binary formation for an asteroid with a rigid core. Snapshot of binary formation for a body with a core of organized large particles (grey), making up $\sim 30\%$ of the total mass, surrounded by smaller particles (white). Shown are two views of the system at the same point in time: looking down the primary spin axis (left; only the primary is shown), and looking along the

plane of the primary's equator and the secondary's orbit (right). The core minimizes equatorial elongation growth, allowing satellite formation. In tests with a smaller core the body becomes very elongated and satellite formation is entirely frustrated.

shape is not initially spherical or oblate, satellite accumulation is delayed until the primary achieves a favourable shape.

The tendency of a gravitational aggregate to adopt an oblate shape as the angular momentum is increased is contrary to the evolution of fluid shapes (the classical Jacobi and MacLaurin figures), which become roughly prolate at rapid rotation rates. Simulations with $\phi \approx 20^\circ$ or $\phi \approx 0^\circ$ behaved most like the classical fluid case. The cases with $\phi \approx 0^\circ$ immediately adopted elongated shapes and maintained prolate shapes during mass loss, frustrating satellite formation for all test parameters. The intermediate test case, with $\phi \approx 20^\circ$, represented a transition, in which binary formation was possible but not very efficient. In our other test case of a substantial rigid core surrounded by smaller, loose particles, the core limited the overall elongation caused by motions of surface material arising from rapid rotation. Thus, a low equatorial elongation was maintained, permitting satellite formation (Fig. 3). Essentially, the minimum requirement for satellite formation is a low equatorial elongation, which was achieved in our models for aggregates with large non-zero angle of friction (which restricts reshaping), or aggregates with a substantial rigid core. In fact, Itokawa, the first asteroid in this size range to be visited by spacecraft, has a morphology suggestive of a large core surrounded by smaller debris¹⁹.

For our nominal case, massive satellites of minimum radius 0.2 primary radii (R_{pri}) formed in all simulations for which the lowest tested value of coefficient of restitution was used (0.2, where 1 is perfectly elastic and 0 is completely dissipative). Efficiency of satellite formation declined as the coefficient of restitution was increased, until, above a value of 0.6, no satellites formed. Evidently satellite accumulation is sensitive to energy dissipation during collisions, suggesting that collisions on the order of $0.2\text{--}0.5\text{ m s}^{-1}$ between asteroidal material dissipate significant amounts of energy. The actual value of the coefficient of restitution during collisions is not well constrained experimentally, but small-scale experiments suggest that it depends on the impact speed and material properties^{20,21}. Values as low as 0.2 can be expected, in particular for bodies with a certain degree of porosity²⁰, such as low-density asteroids and asteroids belonging to dark taxonomic type. Moreover, because the YORP timescale is inversely proportional to density, this model of binary formation is favoured for bodies with low bulk densities or for those consisting of collisionally dissipative materials. However, the YORP timescales are very short compared with dynamical lifetimes, so this mechanism may be indistinguishable between taxonomies. Currently all major taxonomic types are found among the observed binary systems, with no identifiable trends yet.

The exact properties of the secondary and its orbit depend strongly on when the YORP effect ceases to increase the spin of the primary and send mass to the secondary¹⁸. In our simulations, when secondaries grow to $0.3R_{\text{pri}}$, the orbital semimajor axes are between $2.0R_{\text{pri}}$ and $4.5R_{\text{pri}}$, eccentricities are all below 0.15, and the equatorial elongations of the primaries are all below 1.2. Most (70–90%) of the particles

forming the secondary originate from the surface of the primary. After the secondary has formed, 15–35% of the primary's surface is material that originated below the surface and is exposed mostly near the poles of the primary, whereas the equator is still largely covered with original surface material (see Fig. 1). The near absence of observed binary systems with very large secondaries, larger than about half the size of the primary, suggests that mass transfer stops at some point. Our simulations only model the gradual spinup of a single asteroid, and not the additional complex effects that a large secondary in a close orbit may produce, such as the binary YORP effect (BYORP, a radiation effect operating on the system rather than on the primary only), tidal interactions or continued reshaping of the primary. The long-term fate of the system therefore depends on the evolution of the binary, with the BYORP effect or planetary tides possibly splitting the system, leaving behind a rapidly rotating primary¹⁸.

The observed NEA and SMBA binary fraction ($\sim 15\%$) is probably a balance between YORP spinup and known or suspected dynamical sinks (planetary tides and BYORP). The similarities between binaries in the dynamically distinct NEA and SMBA populations arise from their shared minimum physical requirements for binary formation by means of YORP, properties that must be found among a larger population of asteroids that participate in the binary formation–destruction cycle. The requirements include a non-zero angle of friction for the component material (or a rigid core that resists reshaping under stress from rapid rotation), allowing oblate or spherical shapes to be maintained near the critical spin limit, and subsequently permitting the formation of stable satellites (which itself is dependent on a certain degree of collisional dissipation in the component material). These systems may be particularly attractive targets for space missions, because of the exposure of some fresh surface by the movement and removal of surface material from the poles to the equator of the asteroid.

Received 14 March; accepted 29 April 2008.

1. Pravec, P. *et al.* Photometric survey of binary near-Earth asteroids. *Icarus* **181**, 63–93 (2006).
2. Pravec, P. & Harris, A. W. Binary asteroid population. *Icarus* **190**, 250–259 (2007).
3. Ostro, S. J. *et al.* Radar imaging of binary near-Earth asteroid (66391) 1999 KW4. *Science* **314**, 1276–1280 (2006).
4. Scheeres, D. J. *et al.* Dynamical configuration of binary near-Earth asteroid (66391) 1999 KW4. *Science* **314**, 1280–1283 (2006).
5. Richardson, D. C. & Walsh, K. J. Binary minor planets. *Annu. Rev. Earth Planet. Sci.* **34**, 47–81 (2006).
6. Walsh, K. J. & Richardson, D. C. Binary near-Earth asteroid formation: Rubble pile model of tidal disruptions. *Icarus* **180**, 201–216 (2006).
7. Walsh, K. J. & Richardson, D. C. A steady-state model of NEA binaries formed by tidal disruption of gravitational aggregates. *Icarus* **193**, 553–566 (2008).
8. Michel, P. *et al.* Collisions and gravitational reaccumulation: forming asteroid families and satellites. *Science* **294**, 1696–1700 (2001).
9. Durda, D. D. *et al.* The formation of asteroid satellites in catastrophic impacts: Results from numerical simulations. *Icarus* **167**, 382–396 (2004).
10. Rubincam, D. P. Radiative spin-up and spin-down of small asteroids. *Icarus* **148**, 2–11 (2000).

11. Paddack, S. J. & Rhee, J. W. Rotational bursting of interplanetary dust particles. *Geophys. Res. Lett.* **2**, 365–367 (1975).
12. Lowry, S. C. *et al.* Direct detection of the asteroidal YORP effect. *Science* **316**, 272–274 (2007).
13. Taylor, P. A. *et al.* Spin rate of asteroid (54509) 2000 PH5 increasing due to the YORP effect. *Science* **316**, 274–277 (2007).
14. Kaasalainen, M., Durech, J., Warner, B. D., Kugly, Y. N. & Gaftonyuk, N. N. Acceleration of the rotation of asteroid 1862 Apollo by radiation torques. *Nature* **446**, 420–422 (2007).
15. Čuk, M. Formation and destruction of small binary asteroids. *Astrophys. J.* **659**, 57–60 (2007).
16. Pravec, P. & Harris, A. W. Fast and slow rotation of asteroids. *Icarus* **148**, 12–20 (2000).
17. Richardson, D. C., Leinhardt, Z. M., Melosh, H. J., Bottke, W. F. & Asphaug, E. in *Asteroids III* (eds Bottke, W. F. Jr, Cellino, A., Paolicchi, P. & Binzel, R. P.) 501–515 (Univ. of Arizona Press, Tucson, AZ, 2002).
18. Richardson, D. C., Elankumaran, R. E. & Sanderson, R. E. Numerical experiments with rubble piles: equilibrium shapes and spins. *Icarus* **173**, 349–361 (2005).
19. Fujiwara, A. *et al.* The rubble-pile asteroid Itokawa as observed by Hayabusa. *Science* **312**, 1330–1334 (2006).
20. Supulver, K. D., Bridges, F. G. & Lin, D. N. C. The coefficient of restitution of ice particles in glancing collisions: Experimental results for unfrosted surfaces. *Icarus* **113**, 188–199 (1995).
21. Fujii, Y. & Nakamura, A. M. Compaction and fragmentation of porous targets at low velocity collisions. *Lunar Planet. Sci. Conf. XXXVIII*, abstract 1525 (2007).

Acknowledgements We thank W. F. Bottke and A. Harris for their constructive reviews. K.J.W. and D.C.R. acknowledge support from the National Science Foundation under grants AST0307549 and AST0708110. K.J.W. and P.M. also had the support of the European Space Agency's Advanced Concepts Team on the basis of the Ariadna study 07/4111 'Asteroid Centrifugal Fragmentation', and of the French Programme National de Planétologie. K.W. is also supported by the Henri Poincaré fellowship at the Observatoire de la Côte d'Azur, Nice, France. We acknowledge the use of the Mésocentre de Calcul-SIGAMM hosted at the Observatoire de la Côte d'Azur, Nice, France. Some simulations were performed at the University of Maryland with the Department of Astronomy borg cluster and the Office of Information Technology High Performance Computing Cluster. Raytracing for Figs 1 and 3 was performed with the Persistence of Vision Raytracer.

Author Information Reprints and permissions information is available at www.nature.com/reprints. Correspondence and requests for materials should be addressed to K.W. (kwalsh@oca.eu).